

Calvin University

## Calvin Digital Commons

---

University Faculty Publications and Creative Works

University Faculty Scholarship

---

1-1-2000

### Directional correlation in direct and sequential double ionization of model atoms

Stanley L. Haan  
*Calvin University*

N. Hoekema  
*Calvin University*

S. Poniatoski  
*Calvin University*

W. C. Liu  
*National Taiwan Normal University*

Follow this and additional works at: [https://digitalcommons.calvin.edu/calvin\\_facultypubs](https://digitalcommons.calvin.edu/calvin_facultypubs)



Part of the [Optics Commons](#)

---

#### Recommended Citation

Haan, Stanley L.; Hoekema, N.; Poniatoski, S.; and Liu, W. C., "Directional correlation in direct and sequential double ionization of model atoms" (2000). *University Faculty Publications and Creative Works*. 486.

[https://digitalcommons.calvin.edu/calvin\\_facultypubs/486](https://digitalcommons.calvin.edu/calvin_facultypubs/486)

This Article is brought to you for free and open access by the University Faculty Scholarship at Calvin Digital Commons. It has been accepted for inclusion in University Faculty Publications and Creative Works by an authorized administrator of Calvin Digital Commons. For more information, please contact [digitalcommons@calvin.edu](mailto:digitalcommons@calvin.edu).

# Directional correlation in direct and sequential double ionization of model atoms

S.L. Haan, N. Hoekema, S. Poniowski

*Department of Physics and Astronomy, Calvin College,  
Grand Rapids MI 49546 USA*

*haan@calvin.edu*

<http://www.calvin.edu/~haan>

W.-C. Liu

*Department of Physics, National Taiwan Normal University,  
Taipei 116, Taiwan, Republic of China*

J.H. Eberly

*Rochester Theory Center for Optical Science and Engineering,  
and Department of Physics and Astronomy,  
University of Rochester, Rochester NY 14627 USA*

**Abstract:** We discuss directional dependence in the time development of spatial wavefunctions, which includes jet formation, for two-electron model atoms exposed to intense laser fields. Two competing scenarios for double ionization are evident: (1) both electrons emerge simultaneously from the core region and on the same side of the nucleus, and (2) the electrons detach on opposite sides but not simultaneously. The importance of the electron-electron repulsion contribution to the competing processes is investigated for various laser intensities.

© 2000 Optical Society of America

**OCIS codes:** (020.4180) Multiphoton processes (270.6620) Strong-field processes (260.3230) Ionization

---

## References and links

1. D. N. Fittinghof, P. R. Bolton, B. Chang and K. C. Kulander, "Observation of nonsequential double ionization of helium with optical tunneling," *Phys. Rev. Lett.* **69**, 2642 (1992).
2. B. Walker *et al.*, "Precision measurement of strong field double ionization of helium," *Phys. Rev. Lett.* **73**, 1227 (1994).
3. B. Sheehy *et al.*, "Single- and multiple-electron dynamics in the strong-field tunneling limit," *Phys. Rev. A* **58**, 3942 (1999).
4. M.V. Ammosov, N.B. Delone, and V.P. Krainov, "Tunnel ionization of complex atoms and of atomic ions in an alternating electromagnetic field," *Sov. Phys. JETP* **64**, 1191 (1986).
5. S. Larochele, A. Talebpour, and S.L. Chin, "Non-sequential multiple ionization of rare gas atoms in a Ti:Sapphire laser field," *J. Phys. B* **31**, 1201 (1998).
6. A. Becker and F. H. M. Faisal, "Mechanism of laser-induced double ionization of helium," *J. Phys. B* **29**, L197 (1996).
7. F. H. M. Faisal and A. Becker, "Nonsequential double ionization: mechanism and model formula," *Laser Phys.* **7**, 684 (1997).
8. D. Bauer, "Two-dimensional, two-electron model atom in a laser pulse: Exact treatment, single-active-electron analysis, time-dependent density-functional theory, classical calculations, and non-sequential ionization," *Phys. Rev. A* **56**, 3028 (1997).
9. J. B. Watson *et al.*, "Nonsequential Double Ionization of Helium," *Phys. Rev. Lett.* **78**, 1884 (1997).
10. K. Burnett *et al.*, "Multi-electron Response to Intense Laser Fields," *Phil Trans. R. Soc. Lond. A* **356**, 317 (1998).
11. M. S. Pindzola, F. Robicheaux and P. Gavras, "Double multiphoton ionization of a model atom," *Phys. Rev. A* **55**, 1307 (1997).

12. D. G. Lappas and R. Leeuwen, "Electron correlation effects in the double ionization of He," *J. Phys. B* **31**, L249 (1998).
13. W.-C. Liu, J.H. Eberly, S.L. Haan and R. Grobe, "Correlation Effects in Two-Electron Model Atoms in Intense Laser Fields," *Phys. Rev. Lett.* **83**, 520 (1999).
14. J. Parker, K. T. Taylor, C. W. Clark, and S. Blodgett-Ford, "Intense-field multiphoton ionization of a two-electron atom," *J. Phys. B* **29**, L33 (1996).
15. J. Parker, E. S. Smyth, and K. T. Taylor, "Intense-field multiphoton ionization of helium," *J. Phys. B* **31**, L571 (1998).
16. P. B. Corkum, "Plasma perspective on strong field multiphoton ionization," *Phys. Rev. Lett.* **71**, 1994 (1993).
17. Th. Weber *et al.*, "Recoil-Ion Momentum Distributions for Single and Double Ionization of Helium in Strong Laser Fields," *Phys. Rev. Lett.* **84**, 443 (2000).
18. Th. Weber *et al.*, "Sequential and nonsequential contributions to double ionization in strong laser fields," *J. Phys. B* **33**, L127 (2000).
19. Th. Weber *et al.*, "Correlated electron emission in multiphoton double ionization," *Nature* **405**, 658 (2000).
20. R. Moshhammer *et al.*, "Momentum Distributions of  $\text{Ne}^{n+}$  Ions Created by an Intense Ultrashort Laser Pulse," *Phys. Rev. Lett.* **84**, 447 (2000).
21. C. Szymanowski, R. Panfili, W.-C. Liu, S.L. Haan, and J.H. Eberly, "Role of the correlation charge in the double ionization of two-electron model atoms exposed to intense laser fields," *Phys. Rev. A* **61**, 055401 (2000).
22. M.S. Pindzola, D.C. Griffin and C. Bottcher, "Validity of time-dependent Hartree-Fock theory for the multiphoton ionization of atoms," *Phys. Rev. Lett.* **66**, 2305 (1991).
23. R. Grobe and J.H. Eberly, "Photoelectron spectra for a two-electron system in a strong laser field," *Phys. Rev. Lett.* **68**, 2905 (1992).
24. Q. Su and J.H. Eberly, "Model atom for multiphoton physics," *Phys. Rev. A* **44**, 5997 (1991).
25. J.H. Eberly, R. Grobe, C.K. Law and Q. Su, "Numerical experiments in strong and super-strong fields," in *Atoms in Intense Laser Fields*, edited by M. Gavrila, 301 (Academic Press, Boston), 1992.
26. R. Grobe and J.H. Eberly, "One-dimensional model of a negative ion and its interaction with laser fields," *Phys. Rev. A* **48**, 4664 (1993).
27. S.L. Haan, R. Grobe and J.H. Eberly, "Numerical study of autoionizing states in completely correlated two-electron systems," *Phys. Rev. A* **50**, 378 (1994).
28. M. Lein, E.K.U. Gross, and V. Engel, "On the mechanism of strong-field double photoionization in the helium atom," *J. Phys. B* **33**, 433 (2000).
29. M. Dörr, "Double ionization in a one-cycle laser pulse," *Optics Express* **6**, 111 (2000). <http://www.opticsexpress.org/oearchive/source/19114.htm>
30. R. Grobe, S.L. Haan and J. H. Eberly, "A split-domain algorithm for time-dependent multi-electron wave functions," *Comput. Phys. Commun.* **117**, 200 (1999).
31. R. Heather and H. Metiu, "An efficient procedure for calculating the evolution of the wave function by fast Fourier transform methods for systems with spatially extended wave function and localized potential," *J. Chem. Phys.* **86**, 5009 (1987).
32. J.H. Eberly, W.-C. Liu, and S.L. Haan, "The role of correlation in non-sequential double ionization," in press in *Multiphoton Processes*, ed. by J. Keene, L.F. DiMauro, R.R. Freeman, and K.C. Kulander (AIP Press, New York, 2000).

## 1 Introduction

Experimental studies of double ionization of helium atoms in strong laser fields have revealed [1]–[3] a "knee" structure in plots of ionization yield vs. laser intensity. At the highest intensities, the curves correspond to what one would expect for sequential ionization of non-interacting electrons, i.e., the systems exhibit Ammosov-Delone-Krainov (ADK) behavior [4, 5]. At lower intensities, however, there is a greater amount of ionization than would be expected for uncorrelated electrons. These experimental studies have drawn considerable theoretical interest as researchers seek to understand the nature of the "excess" double ionization [6]–[16]. Recent experimental reports [17]–[20] of electrons emerging on the same side of the nucleus provide further data to challenge theoretical work.

Because of the complexity of a two-electron, three-dimensional system, many theoretical groups have been working with a reduced-dimensionality model of the helium

atom [11], [22]–[29]. This model allows the use of fully two-electron wavefunctions in numerical studies of the ionization process. In this model the electrons and (fixed) nucleus interact via a 1-D screened Coulomb potential [24, 25]. In atomic units, the Hamiltonian for “one dimensional helium” interacting with an external laser field can be written

$$H(x, y) = \frac{p_x^2}{2} + \frac{p_y^2}{2} - \frac{2}{\sqrt{x^2 + 1}} - \frac{2}{\sqrt{y^2 + 1}} + \frac{C}{\sqrt{(x - y)^2 + 1}} + W(x, y, t) \quad (1)$$

Here  $x$  and  $y$  denote position variables for the electrons, and  $C$  represents a “correlation charge.” We typically set  $C = 1$  so that the electron-electron interaction is of equal strength with the electron-proton interaction, but variation of  $C$  also can provide information about electron correlation.

The interaction with the laser field is

$$W(x, y, t) = -(x + y)E_0 f(t) \sin \omega t \quad (2)$$

Here  $E_0$  denotes the field strength,  $\omega$  the laser frequency, and  $f(t)$  is a pulse-shape parameter, which we take to be trapezoidal.

In our numerical investigations we discretize the  $x$  and  $y$  variables, and solve the Schrödinger equation on the resulting two-coordinate spatial grid. We evolve the spatial wavefunction  $\Psi(x, y)$  in time using split-operator techniques and a split-domain algorithm [26, 30, 31]. We begin with the system in its ground state, which we assume to be spin zero. Consequently the initial spatial wavefunction is symmetric with respect to exchange of the electrons. Then because  $H$  contains no spin-dependent interactions, this exchange symmetry  $\Psi(x, y) = \Psi(y, x)$  is preserved for all time.

It is known [13] that for this model system the double-ionization probability, when considered as a function of laser intensity, shows a knee structure qualitatively similar to what is observed experimentally. Further, the height of the knee depends critically on the value of the correlation charge  $C$  [21], supporting the conjecture that non-ADK behavior arises because of an interaction between the electrons.

We have previously shown [32] that the spatial wavefunction for the two-electron system exhibits jets of double ionization each half cycle, provided the laser has reached sufficient strength and enough time has elapsed for recollision to occur. In these jets, the two electrons emerge simultaneously on the same side of the nucleus. We have found that for laser intensities corresponding to the “knee” area, the size of the jets is very dependent on the correlation charge  $C$  [13]. In addition, we have noted that there is a competing double-ionization process in which the electrons emerge sequentially on opposite sides of the nucleus, and we have commented that the sequential ionization apparently dominates at intensities above the knee.

Finally, we should note other recent progress in the field. There is now strong experimental evidence [17]–[20] of having both electrons emerge on the same side of the nucleus. This evidence is based on a momentum analysis of outgoing particles, and is consistent with the two-electron jets. Other theoretical results showing the double-ionization jets have also recently appeared [28, 29].

## 2 Time Development of the Spatial Wavefunction

We begin by examining the general characteristics of the time development of the spatial wavefunction. We look in particular at a four-cycle  $1 + 2 + 1$  trapezoidal pulse of peak intensity  $I = 6.5 \times 10^{14} W/cm^2$  with its frequency corresponding to five-photon single ionization. This frequency places the ionization in the knee area [13].

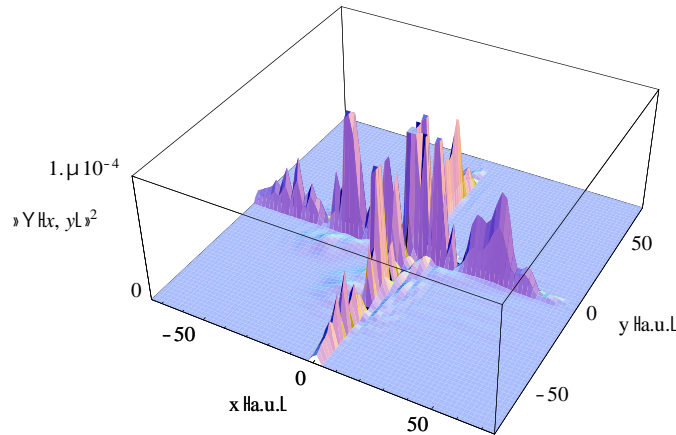


Fig. 1. Animation (0.9 MB) of the time development of  $|\Psi(x, y)|^2$  for one-dimensional helium for a four-cycle pulse of intensity  $6.5 \times 10^{14} W/cm^2$  and frequency  $0.1837 a.u.$ . The still image is for  $t = 2.875$  cycles and shows the jets as well as sequential ionization.

Figure 1 presents a QuickTime video of the time development of the modulus squared of the spatial wavefunction. We truncate the plot vertically at  $10^{-4}$  for the clearest viewing of the general characteristics of the development. We have previously presented [32] logarithmic contour plots for this time development, but with much larger time increments. The animation shows 32 images per cycle. The still image in Fig. 1 is for  $t=2.875$  cycles.

A conspicuous characteristic of the development is the oscillation of the wavefunction in response to the external field. When  $x$  and  $y$  coordinates are plotted orthogonally as in Fig. 1, the interaction (2) is equivalent to having an electric field pointing alternately parallel and antiparallel to the line  $y = x$ .

Single ionization, which is characterized by population moving steadily outward along the  $x$  and  $y$  axes, is clearly evident. Since the field oscillations can bring the population back to the core region, considerable rescattering occurs.

Double ionization is evident when population separates from the axes, and ripples of double ionization are visible in Fig. 1. In Fig. 2 we change the viewpoint, and show the jets at  $t = 2.25$  cycles. The jets emerge during the latter part of each half cycle and in the direction of electric force. Their emergence directly from the origin indicates simultaneous departure from the nuclear region for the two electrons (although this need not be the first departure for both!); their direction of motion implies that the electrons have similar velocities. (Motion directly along the line  $y = x$  would correspond to equal velocities.) The  $x - y$  symmetry mentioned above is obvious.

Once the electrons are away from the core region the repulsive force between the electrons causes them to separate. In our 1-D system the combined effect of the electric field and the electron-electron repulsion is to send population out of the first and third quadrants and into the second and fourth quadrants, i.e., to send one electron back across the nucleus. In a three dimensional system one could also expect the electron-electron repulsion to cause the emerging electrons to separate. Of course, the appearance of electrons on the same side of the nucleus is completely consistent with recent reports of electron momentum correlation [17]–[20].

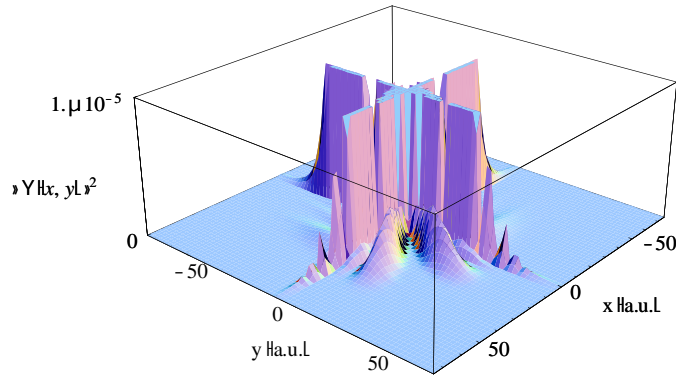


Fig. 2. Animation (1.0 MB) of the time development of  $|\Psi(x, y)|^2$  as for Fig. 1, but viewed from along the line  $y = x$ , and truncated at  $10^{-5}$ . The still image is for  $t = 2.25$  cycles.

It is noteworthy that jets do not emerge in the first quadrant until the second half of the second cycle even though there is considerable population along the axes during the first half of the cycle. This suggests that rescattering is important in the formation of the jets. The apparent inertial effects that they show are also consistent with a rescattering interpretation.

In [32] we also noted that the jets are not the only method of double ionization. There is more population emerging in the second and fourth quadrants than can be accounted for by the jets. As can be seen in Fig. 1 for times near 1.875 cycles and 2.875 cycles, some doubly-ionized population apparently emerges from the axes rather than directly from the origin. This population can be associated with sequential double ionization. It is interesting to observe, however, that these population bursts appear to travel perpendicular to the axes, suggesting that the outer electron is nearly at rest when the inner electron is ionized.

We thus see clearly that there is a competition between different processes of double ionization, and one might expect that the different processes would depend differently on variables such as laser field strength and the strength of the electron-electron repulsion. One of the results of [13] was that the strength of the double-ionization signal in the vicinity of the knee is highly dependent on the value of the correlation  $C$  appearing in the Hamiltonian 1. Our detailed plots allow us to investigate reasons underlying this dependence.

We have studied the time development of the system with  $C = 0.9$  or  $C = 1.1$  to complement our studies with  $C = 1.0$ . Figures 3 and 4 show logarithmic contour plots of  $|\Psi(x, y)|^2$  vs.  $x$  and  $y$  after each cycle of 6-cycle (2+2+2 trapezoidal) pulse for the three values of  $C$ . Other parameters are the same as for Figs. 1 and 2. Because of the longer turn-on time, no significant double ionization occurs until the third laser cycle. These plots show a considerable increase in double ionization with increasing  $C$ . The enhancement of the jets with increased  $C$  is especially noteworthy.

To examine in more detail the enhancement of the jets that occurs when  $C$  is increased, Fig. 5 repeats Fig. 2, but with  $C=1.1$ . The enhancement of the jets with in-

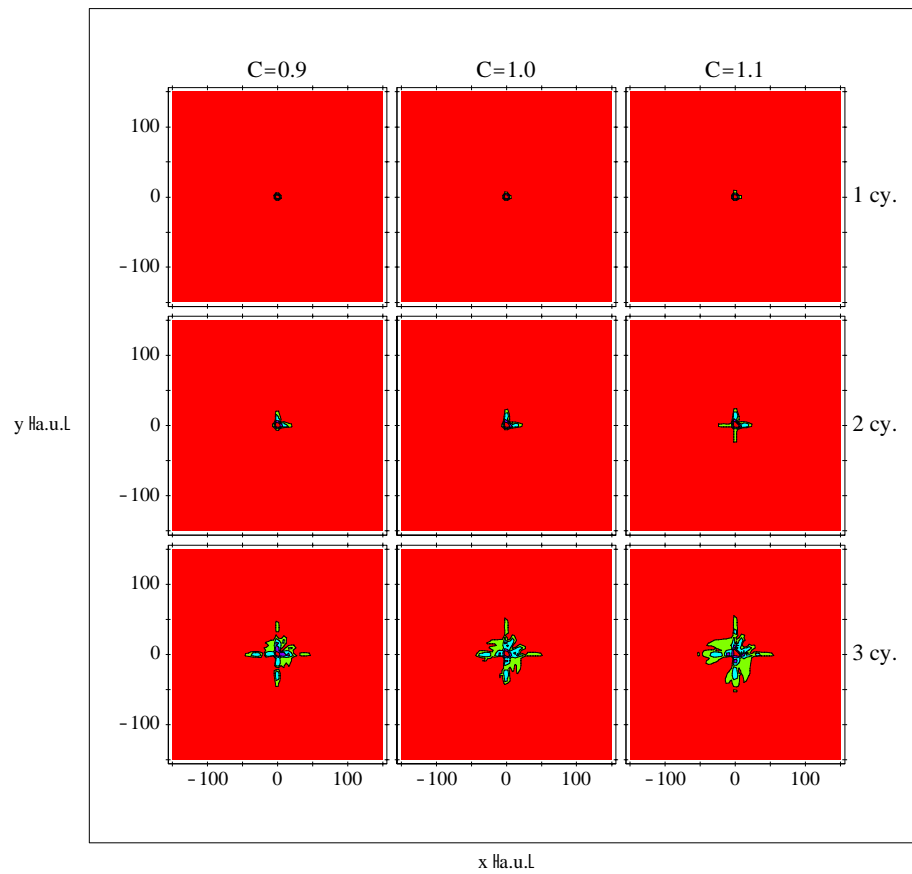


Fig. 3. Logarithmic contour plots of  $|\Psi(x,y)|^2$  vs.  $x$  and  $y$  after each of the first three cycles of a 6-cycle (2+2+2 trapezoidal) pulse for  $C = 0.9, 1.0,$  and  $1.1$ . Other parameters are the same as for Figs. 1 and 2.

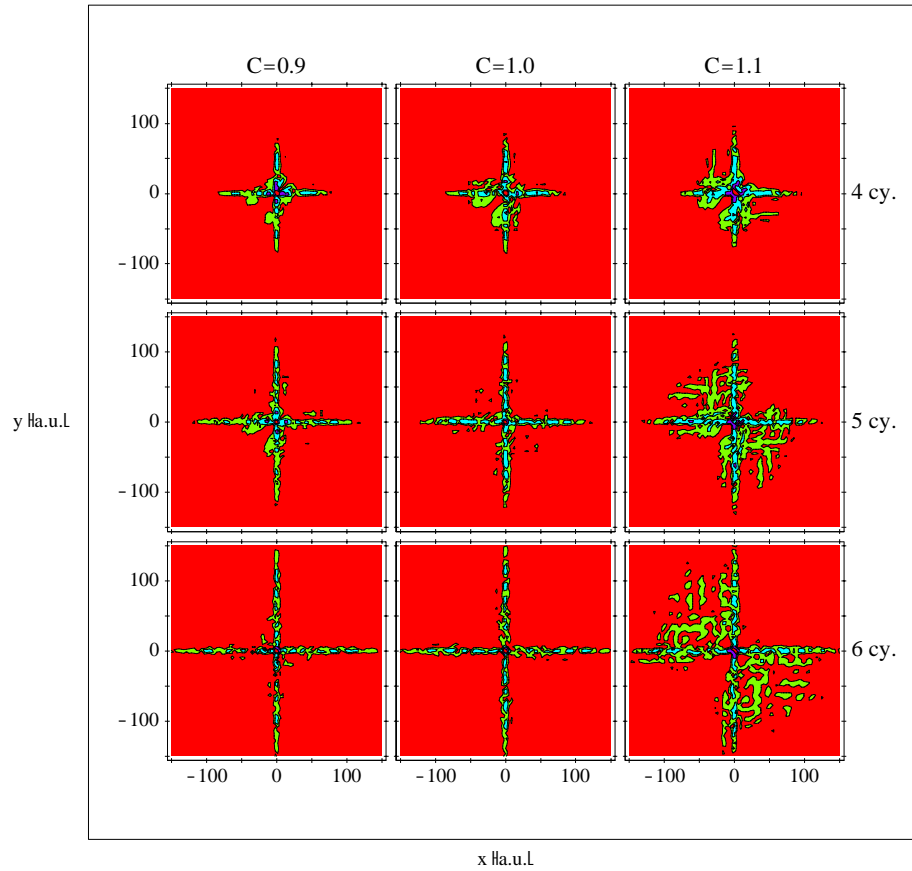


Fig. 4. Continuation of Fig. 3, showing  $|\Psi(x, y)|^2$  vs.  $x$  and  $y$  after each of the final three cycles of a 6-cycle (2+2+2 trapezoidal) pulse for  $C = 0.9, 1.0,$  and  $1.1$ .

creased correlation charge  $C$  is very dramatic.

In order to consider next the dependence of sequential ionization on the correlation charge  $C$ , in Fig. 6 we present still images of  $|\Psi(x, y)|^2$  at  $t = 1.875$  cycles for the two  $C$  values from the same viewpoint as in Fig. 1. There is an enhancement of the sequential ionization, but not as dramatic as the jet enhancement. The inference we draw is what might have been expected, namely that the electron-electron repulsion is not as important in the sequential ionization as for rescattering ionization.

Figures 3 through 6 suggest that the reason for the strong dependence of the knee on correlation charge  $C$ —and hence the reason for the enhanced double ionization—is the jets.

To test this inference regarding the importance of the jets, we now turn our attention to a higher laser intensity, namely  $1.0 \times 10^{15} \text{ W/cm}^2$ . We keep the same laser frequency. Figure 7 is analogous to Fig. 1, but for this higher laser intensity. Enhancement is clearly visible for the jets as well as for the sequential ionization, but increasing the laser intensity has clearly had greater effect on the sequential ionization than on the jets. This result is consistent with our expectation that sequential ionization should become more dominant as the laser intensity is increased.

We have previously shown that the total ionization probability becomes less dependent on  $C$  at intensities above the knee. This conclusion is supported by Figs. 8 and



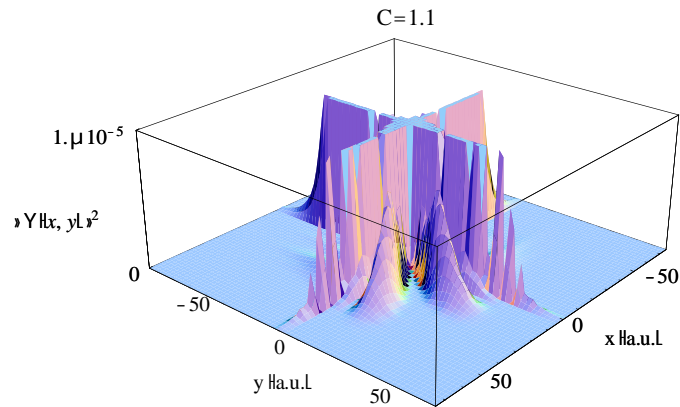


Fig. 5. Animation (1.7 MB) of the time development of  $|\Psi(x, y)|^2$  as for Fig. 2, but with correlation charge  $C = 1.1$  instead of 1.0. The still image shows  $|\Psi(x, y)|^2$  at  $t = 2.25$  cycles.

9, which compare stop-action views for  $C = 1.0$  and 1.1, and shows that increased  $C$  provides noticeable enhancement of the jets. Figure 9 shows the sequential ionization at  $t = 1.875$  cycles for the two values of  $C$ , and shows once again that the sequential ionization is less dependent on  $C$  than the jets are. All these results are consistent with the idea that the knee is due to the double-ionization jets. At high intensities such as that of Figs. 7-9, the sequential ionization begins to dominate.

Finally, we consider a lower intensity,  $I = 3 \times 10^{14} W/cm^2$ , which is below the knee area. In Figs. 10, we present stop-action shots (for  $C = 1.0$ ) at times  $t = 1.875$  cycles (left) and  $t = 2.25$  cycles (right). Because of diminished ionization, the plots use vertical scales that are a factor of 10 lower than in our earlier figures. At this intensity, the jets are more visible than the sequential double ionization. These times are the same as for earlier plots.

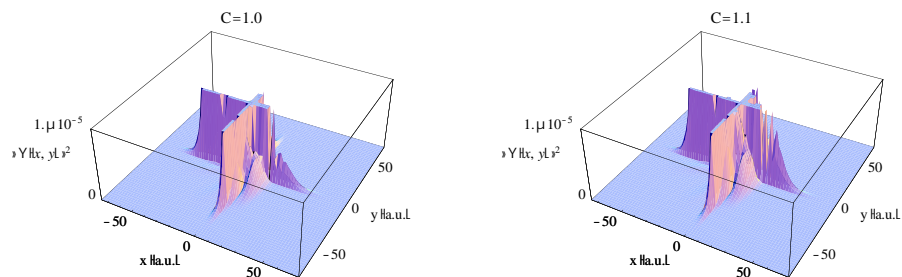


Fig. 6. Linear plots of  $|\Psi(x, y)|^2$  vs.  $x$  and  $y$  at  $t = 1.875$  cycles for  $C = 1.0$  and 1.1, showing only small enhancement of the sequential ionization for increased  $C$ . Laser parameters are as for Figs. 1-5.

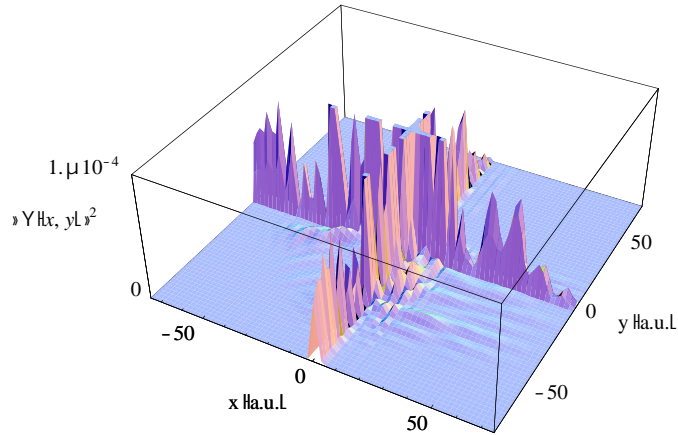


Fig. 7. Animation (1.0 MB) of the time development of  $|\Psi(x, y)|^2$  for one-dimensional helium for a four-cycle trapezoidal pulse (1+2+1) of intensity  $1.0 \times 10^{15} \text{ W/cm}^2$  and frequency  $0.1837 \text{ a.u.}$ . The still image is for  $t=2.875$  cycles, and shows both jets and sequential ionization.

### 3 Summary

We have examined numerical results for the time development of one-dimensional helium exposed to intense laser light. We have considered three laser intensities—one below the knee, one at the knee, and one above the knee.

Our data makes clear that there are competing processes for double ionization. In one process, which we assign to rescattering, the two electrons emerge from the core simultaneously and on the same side of the nucleus in “jets”. We have seen that these double-ionization jets are particularly sensitive to the strength of the electron-electron interaction in the knee area. We conclude that these double ionization jets are responsible for the enhanced double ionization that leads to the knee.

We have also examined a competing process of double ionization, in which the electrons leave the nuclear area sequentially. We have noted that electron-electron repulsion still plays a role in this process, since the electrons emerge on opposite sides of the nucleus. However, this process is not as sensitive to small changes in the electron-electron

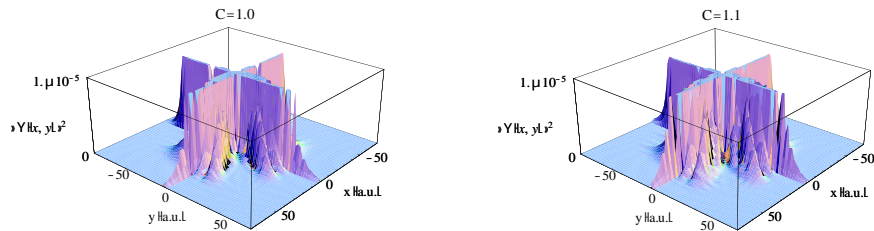


Fig. 8. Linear plots of  $|\Psi(x, y)|^2$  vs.  $x$  and  $y$  at  $t = 2.25$  cycles for  $C = 1.0$  and  $1.1$ , and for laser parameters of Fig 7. As for the lower intensity, there is an enhancement of the double-ionization jets.

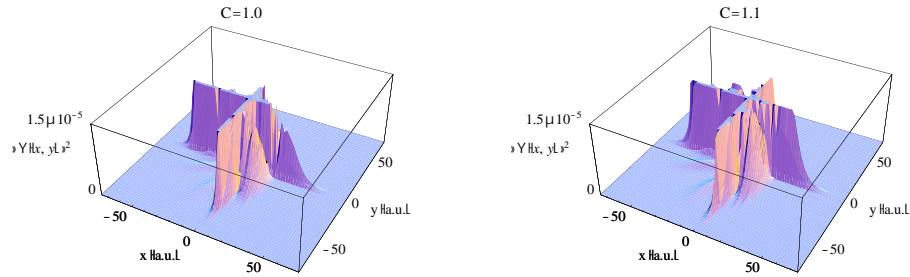


Fig. 9. Linear plots of  $|\Psi(x, y)|^2$  vs.  $x$  and  $y$  at  $t = 1.875$  cycles for  $C = 1.0$  and  $1.1$ , and laser parameters as in Figs. 7-8. Note that the vertical axis is truncated at larger values than in Fig. 8. At this intensity the sequential ionization begins to dominate the double-ionization jets.

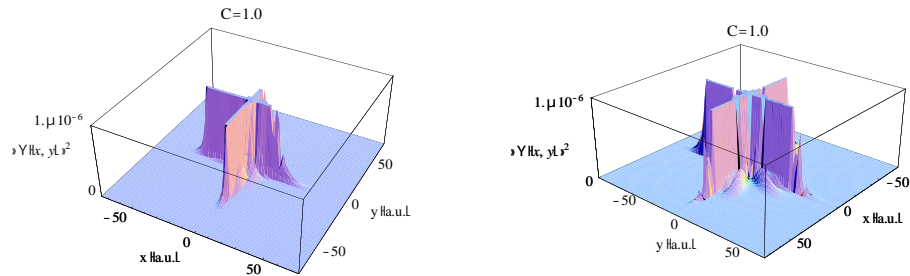


Fig. 10. Linear plots of  $|\Psi(x, y)|^2$  vs.  $x$  and  $y$  at  $t = 1.875$  cycles (left) and  $t = 2.25$  cycles (right) for  $C = 1.0$ , and laser intensity  $3.0 \times 10^{14} W/cm^2$ . The laser frequency remains unchanged from earlier plots, and is  $0.1837 a.u.$ . The two plots have very different viewpoints.

repulsion as the jets are. Further, we have found that this process increases more rapidly with laser intensity than the double-ionization jets, and totally dominates at high intensities.

The use of detailed videos of the time-development of  $|\Psi(x, y)|^2$  is useful in developing understanding of the single and double-ionization process. One topic we have not discussed is the the role that resonances might play in the ionization process. Changing the value of  $C$  will also change energy-levels of the model system, which can alter the dynamics of the double-ionization process. Some of us take up that topic elsewhere [21].

### Acknowledgements

This work has been supported by the National Science Foundation through Grants PHY-9415583 to the University of Rochester and PHY-9722079 to Calvin College, and by Calvin College. We acknowledge the assistance of R. Panfili and C. Szymanowski.